



C. Steve Suh | Meng-Kun Liu

Control of Cutting Vibration and Machining Instability

A Time-Frequency Approach for
Precision, Micro and Nano Machining

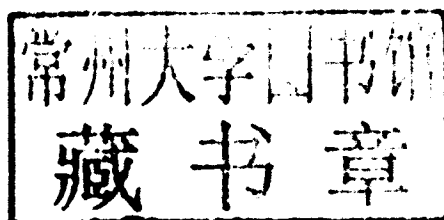
 **WILEY**

CONTROL OF CUTTING VIBRATION AND MACHINING INSTABILITY

**A TIME-FREQUENCY APPROACH
FOR PRECISION, MICRO AND
NANO MACHINING**

C. Steve Suh and Meng-Kun Liu

Texas A&M University, USA



 **WILEY**

A John Wiley & Sons, Ltd., Publication

This edition first published 2013
© 2013 John Wiley & Sons, Ltd

Registered office

John Wiley & Sons Ltd, The Atrium, Southern Gate, Chichester, West Sussex, PO19 8SQ, United Kingdom

For details of our global editorial offices, for customer services and for information about how to apply for permission to reuse the copyright material in this book please see our website at www.wiley.com.

The right of the author to be identified as the author of this work has been asserted in accordance with the Copyright, Designs and Patents Act 1988.

All rights reserved. No part of this publication may be reproduced, stored in a retrieval system, or transmitted, in any form or by any means, electronic, mechanical, photocopying, recording or otherwise, except as permitted by the UK Copyright, Designs and Patents Act 1988, without the prior permission of the publisher.

Wiley also publishes its books in a variety of electronic formats. Some content that appears in print may not be available in electronic books.

Designations used by companies to distinguish their products are often claimed as trademarks. All brand names and product names used in this book are trade names, service marks, trademarks or registered trademarks of their respective owners. The publisher is not associated with any product or vendor mentioned in this book.

Limit of Liability/Disclaimer of Warranty: While the publisher and author have used their best efforts in preparing this book, they make no representations or warranties with respect to the accuracy or completeness of the contents of this book and specifically disclaim any implied warranties of merchantability or fitness for a particular purpose. It is sold on the understanding that the publisher is not engaged in rendering professional services and neither the publisher nor the author shall be liable for damages arising herefrom. If professional advice or other expert assistance is required, the services of a competent professional should be sought.

MATLAB[®] is a trademark of The MathWorks, Inc. and is used with permission. The MathWorks does not warrant the accuracy of the text or exercises in this book. This book's use or discussion of MATLAB[®] software or related products does not constitute endorsement or sponsorship by The MathWorks of a particular pedagogical approach or particular use of the MATLAB[®] software.

Library of Congress Cataloging-in-Publication Data

Suh, C. Steve

Control of cutting vibration and machining instability : a time-frequency approach for precision, micro and nano machining / C. Steve Suh and Meng-Kun Liu.

pages cm

Includes bibliographical references and index.

ISBN 978-1-118-37182-4 (cloth)

1. Cutting-Vibration. 2. Machine-tools-Vibration. 3. Machining. 4. Machinery, Dynamics of.
5. Time-series analysis. 6. Microtechnology 7. Nanotechnology. I. Liu, Meng-Kun. II. Title.
TJ1186.S86 2013
671.3'5-dc23

2013014158

A catalogue record for this book is available from the British Library

ISBN: 9781118371824

Typeset in 10/12pt Times by Aptara Inc., New Delhi, India

Printed and bound in Singapore by Markono Print Media Pte Ltd

Preface

Controllers are either designed in the frequency domain or time domain. When designed in the frequency domain, it is a common practice that a transfer function is derived from the corresponding governing equation of motion. Frequency response design methods, such as bode plots and root loci, are usually employed for the design of frequency domain based controllers. When designed in the time domain, the differential equation of the system is described as a state space model by the associated state variables. The controllability and observability of the design are then investigated using state feedback or other time domain control laws. Controllers designed in either domain have their advantages. Controllers designed in the frequency domain provide adequate performance with uncertainties. Estimating the output phase and amplitude in response to a sinusoidal input is generally sufficient to design a feedback controller, but the system has to be linear and stationary. Controllers designed in the time domain can accommodate multiple inputs-outputs and correlate internal and external states without considering the requirements in the frequency domain. Proven feasible for linear, stationary systems, both types of controllers can only be applied independently either in the frequency domain or the time domain.

For a linear time-invariant system, only the amplitude and phase angle of the input are changed by the system. The output frequency remains the same as the input frequency, and the system can be stabilized by applying a proper feedback gain. Both the time domain and frequency domain responses are bounded at the same time. However, this is not the case for the chaotic response generated by a nonlinear system. A chaotic response is naturally bounded in the time domain while becoming unstably broadband in the frequency domain, containing an infinite number of unstable periodic orbits of all periods in the phase portrait, called strange attractors. It does not remain in one periodic orbit but switches rapidly between these unstable periodic orbits. If the chaotic response is projected onto the Poincaré section, a lower dimensional subspace transversal to the trajectory of the response, numerous intersection points would be seen densely congregating and being confined within a finite area. This unequivocally implies that the chaotic response is bounded within a specific range in the time domain and dynamically deteriorates at the same time with a changing spectrum of broad bandwidth as the trajectory switching rapidly between infinite numbers of unstable periodic orbits. This phenomenon is prevalent in high-speed cutting operations where strong nonlinearities including regenerative effects, frictional discontinuity, chip formation, and tool stiffness are dominant.

For a nonlinear, nonstationary system, when it undergoes bifurcation to eventual chaos, its time response is no longer periodic. Broadband spectral response of additional frequency

components emerge as a result. Controllers designed in the time domain contain time-domain error while being unable to restrain the increasing bandwidth. On the other hand, controllers designed in the frequency domain restrict the bandwidth from expanding while losing control over the time domain error. Neither frequency domain nor time domain based controllers are sufficient to address aperiodic response and route-to-chaos. This is further asserted by the uncertainty principle, which states that the resolution in the time- and frequency-domain cannot be reached arbitrarily. However, as Parseval's Theorem implies that the energies computed in the time- and frequency-domains are interchangeable, it is possible to incorporate and meet the time and frequency domain requirements together and realize the control of a nonlinear response with reconciled, concurrent time-frequency resolutions.

The above is a concise version of what was on our mind when we contemplated many years ago the following two questions: (1) *Why is it that a dynamic response could be bounded in the time domain while in the meantime becoming unstably broadband in the frequency domain simultaneously?* and (2) *Why is it that the control of a nonlinear system has to be performed in the simultaneous time-frequency domain to be viable and effective?* The wavelet-based time-frequency control methodology documented in this monograph is the embodiment of our response to these particular questions.

The control methodology is adaptive in that it monitors and makes timely and proper adjustments to improve its performance. Plant parameters in the novel control are identified in real-time and are used to adjust and update the control laws according to the changing system output. Its architecture is inspired by active noise control in which one FIR filter identifies the system and another auto-adjustable FIR filter rejects the uncontrollable input. Analysis wavelet filter banks are incorporated in the control configuration. The analysis filter banks decompose both input and error signals before the controlled signal is synthesized. As a dynamic response is resolved by the discrete wavelet transform into components at various scales corresponding to successive octave frequencies, the control law is inherently built in the joint time-frequency domain, thus facilitating simultaneous time-frequency control. Unlike active noise control whose objective is to reduce acoustic noise, the wavelet-based time-frequency control is designed to minimize the deterioration of the output signal in both the time and frequency domains when the system undergoes bifurcated or chaotic motion so as to restore the output response to periodic. These features together provide unprecedented advantages for the control of nonlinear, nonstationary system response.

This book presents a sound foundation which engineering professionals, practicing and in training alike, can rigorously explore to realize important progress in micro-manufacturing, precision machine-tool design, and chatter control. Viable solution strategies can be formulated drawing from the foundation to control cutting instability at high speed and to develop chatter-free machine-tool concepts. Research professionals in the general areas of nonlinear dynamics and nonlinear control will also find the volume informative in qualitative and quantitative terms on how discontinuity and chaos can be adequately mitigated.

The discourse of *Control of Cutting Vibration and Machining Instability* is organized into eleven chapters. The first chapter examines the coupled tool-workpiece interaction for a better understanding of the instability and chatter in turning operation. The second chapter is a brief review of the mathematical basics along with the common notations relevant to the derivation of the wavelet-based nonlinear time-frequency control law in Chapter 7. The third chapter reviews the essences of active noise control and the filtered-x LMS algorithm that are incorporated in the time-frequency control as features for system identification and

error reduction. The notion of time-frequency analysis is discussed in the fourth chapter. This chapter presents several analysis tools important for the proper characterization of nonlinear system responses. It also lays the fundamentals needed to comprehend wavelet filter banks and the underlying concept of time-frequency resolution that are treated in the chapter that follows, Chapter 5.

The philosophical basis on which the nonlinear time-frequency control is based is elaborated in greater detail in Chapter 6. Chapter 7 presents the time-frequency control theory along with all the salient physical features that render chaos control feasible. The feasibility is demonstrated in applications in Chapters 8 through 11 using examples from high-speed manufacturing and friction-induced discontinuity. The last chapter, Chapter 11, explores an alternative solution to mitigating chaos using the time-frequency control. The implication for exploring synchronization of chaos to achieve suppressing self-sustained chaotic machining chatter is emphasized.

Two working MATLAB® *m*-files by which all the results and figures in Chapters 10 and 11 are generated are listed in the Appendix. The one for the friction-induced instability control in Chapter 10 has an extensive finite element coding section in it that utilizes several user-defined MATLAB® functions in Simulink® for the calculation of the beam vibration. We hope the examples will encourage the gaining of practical experience in implementing the wavelet-based nonlinear time-frequency control methodology. Readers who are reasonably familiar with the MATLAB® language and Simulink simulation tool should find the examples extensive, complete, and easy to follow.

Since it was first conceived years ago, many talented individuals have come along and helped evolve the core ideas of time-frequency control. Among them are Baozhong Yang, who explored instantaneous frequency as the tool of preference for characterizing nonlinear systems, and Achala Dassanayake, to whom we owe the comprehensive understanding of what machining instability and chatter really are.

C. Steve Suh and Meng-Kun Liu
Texas A&M University, College Station, USA
February 2013

Contents

| | |
|---|-----------|
| Preface | ix |
| 1 Cutting Dynamics and Machining Instability | 1 |
| 1.1 Instability in Turning Operation | 2 |
| 1.1.1 Impact of Coupled Whirling and Tool Geometry on Machining | 3 |
| 1.2 Cutting Stability | 10 |
| 1.3 Margin of Stability and Instability | 12 |
| 1.4 Stability in Fine Cuts | 23 |
| 1.5 Concluding Remarks | 31 |
| References | 32 |
| 2 Basic Physical Principles | 33 |
| 2.1 Euclidean Vectors | 33 |
| 2.2 Linear Spaces | 34 |
| 2.3 Matrices | 36 |
| 2.3.1 Eigenvalue and Linear Transformation | 37 |
| 2.4 Discrete Functions | 38 |
| 2.4.1 Convolution and Filter Operation | 39 |
| 2.4.2 Sampling Theorem | 40 |
| 2.4.3 z-Transform | 41 |
| 2.5 Tools for Characterizing Dynamic Response | 42 |
| 2.5.1 Fourier Analysis | 49 |
| 2.5.2 Wavelet Analysis | 51 |
| References | 54 |
| 3 Adaptive Filters and Filtered-x LMS Algorithm | 55 |
| 3.1 Discrete-Time FIR Wiener Filter | 55 |
| 3.1.1 Performance Measure | 56 |
| 3.1.2 Optimization of Performance Function | 58 |
| 3.2 Gradient Descent Optimization | 60 |
| 3.3 Least-Mean-Square Algorithm | 62 |
| 3.4 Filtered-x LMS Algorithm | 64 |
| References | 68 |

| | | |
|----------|--|------------|
| 4 | Time-Frequency Analysis | 71 |
| 4.1 | Time and Frequency Correspondence | 72 |
| 4.2 | Time and Frequency Resolution | 75 |
| 4.3 | Uncertainty Principle | 76 |
| 4.4 | Short-Time Fourier Transform | 77 |
| 4.5 | Continuous-Time Wavelet Transform | 79 |
| 4.6 | Instantaneous Frequency | 81 |
| 4.6.1 | Fundamental Notions | 82 |
| 4.6.2 | Misinterpretation of Instantaneous Frequency | 85 |
| 4.6.3 | Decomposition of Multi-Mode Structure | 90 |
| 4.6.4 | Example of Instantaneous Frequency | 94 |
| 4.6.5 | Characteristics of Nonlinear Response | 97 |
| | References | 100 |
| 5 | Wavelet Filter Banks | 101 |
| 5.1 | A Wavelet Example | 101 |
| 5.2 | Multiresolution Analysis | 104 |
| 5.3 | Discrete Wavelet Transform and Filter Banks | 112 |
| | References | 116 |
| 6 | Temporal and Spectral Characteristics of Dynamic Instability | 117 |
| 6.1 | Implication of Linearization in Time-Frequency Domains | 118 |
| 6.2 | Route-to-Chaos in Time-Frequency Domain | 125 |
| 6.3 | Summary | 134 |
| | References | 134 |
| 7 | Simultaneous Time-Frequency Control of Dynamic Instability | 137 |
| 7.1 | Property of Route-to-Chaos | 137 |
| 7.1.1 | OGY Control of Stationary and Nonstationary Hénon Map | 139 |
| 7.1.2 | Lyapunov-based Control of Stationary and Nonstationary Duffing Oscillator | 140 |
| 7.2 | Property of Chaos Control | 144 |
| 7.2.1 | Simultaneous Time-Frequency Control | 145 |
| 7.3 | Validation of Chaos Control | 155 |
| | References | 162 |
| 8 | Time-Frequency Control of Milling Instability and Chatter at High Speed | 165 |
| 8.1 | Milling Control Issues | 165 |
| 8.2 | High-Speed Low Immersion Milling Model | 167 |
| 8.3 | Route-to-Chaos and Milling Instability | 168 |
| 8.4 | Milling Instability Control | 170 |
| 8.5 | Summary | 175 |
| | References | 176 |
| 9 | Multidimensional Time-Frequency Control of Micro-Milling Instability | 177 |
| 9.1 | Micro-Milling Control Issues | 177 |
| 9.2 | Nonlinear Micro-Milling Model | 179 |

| | | |
|---|---|------------|
| 9.3 | Multivariable Micro-Milling Instability Control | 181 |
| 9.3.1 | Control Strategy | 183 |
| 9.4 | Micro-Milling Instability Control | 186 |
| 9.5 | Summary | 193 |
| | References | 197 |
| 10 | Time-Frequency Control of Friction Induced Instability | 199 |
| 10.1 | Issues with Friction-Induced Vibration Control | 199 |
| 10.2 | Continuous Rotating Disk Model | 201 |
| 10.3 | Dynamics of Friction-Induced Vibration | 206 |
| 10.4 | Friction-Induced Instability Control | 208 |
| 10.5 | Summary | 214 |
| | References | 215 |
| 11 | Synchronization of Chaos in Simultaneous Time-Frequency Domain | 217 |
| 11.1 | Synchronization of Chaos | 217 |
| 11.2 | Dynamics of a Nonautonomous Chaotic System | 219 |
| 11.3 | Synchronization Scheme | 222 |
| 11.4 | Chaos Control | 223 |
| | 11.4.1 Scenario I | 223 |
| | 11.4.2 Scenario II | 227 |
| 11.5 | Summary | 227 |
| | References | 229 |
| Appendix: MATLAB® Programming Examples of Nonlinear Time-Frequency Control | | 231 |
| A.1 | Friction-Induced Instability Control | 231 |
| | A.1.1 Main Program | 232 |
| | A.1.2 Simulink® Model | 236 |
| A.2 | Synchronization of Chaos | 239 |
| | A.2.1 Main Program | 239 |
| | A.2.2 Simulink® Model | 244 |
| Index | | 245 |

1

Cutting Dynamics and Machining Instability

Material removal – as the most significant operation in manufacturing industry – is facing the ever-increasing challenge of increasing proficiency at the micro and nano scale levels of high-speed manufacturing. Fabrication of submicron size three-dimensional features and freeform surfaces demands unprecedented performance in accuracy, precision, and productivity. Meeting the requirements for significantly improved quality and efficiency, however, are contingent upon the optimal design of the machine-tools on which machining is performed. Modern day precision machine-tool configurations are in general an integration of several essential components including process measurement and control, power and drive, tooling and fixture, and the structural frame that provides stiffness and stability. As dynamic instability is inherently prominent and particularly damaging in high-speed precision cutting, *design for dynamics* is favored for the design of precision machine tool systems [1]. This approach employs computer-based analysis and design tools to optimize the dynamic performance of machine-tool design at the system level. It is largely driven by a critical piece of information – the vibration of the machine-tool. Due to the large set of parameters that affect cutting vibrations, such as regenerative effects, tool nonlinearity, cutting intermittency, discontinuous frictional excitation, and environmental noise, among many others, the effectiveness of the approach commands that the dynamics of machining be completely established throughout the entire process.

This book explores the fundamentals of cutting dynamics to the formulation and development of an innovative control methodology. The coupling, interaction, and evolution of different cutting states are studied so as to identify the underlying critical parameters that can be controlled to negate machining instability and enable better machine-tool design for precision micro and nano manufacturing.

The main features that contribute to the robust control of cutting instability are: (1) comprehension of the underlying dynamics of cutting and interruptions in cutting motions, (2) operation of the machine-tool system over a broad range of operating conditions with

minimal vibration, such as high-speed operation to achieve a high-quality finish of the machined surface, (3) an increased rate of production to maximize profit and minimize operating and maintenance costs, (4) concentration on the apparent discontinuities that allows the nature of the complex machine-tool system motions to be fully established. The application of simultaneous time-frequency nonlinear control to mitigate complex intermittent cutting is both novel and unique. The impact on the area of material removal processes is in the mitigation of cutting instability and chaotic chattering motion induced by frictional and tool nonlinearity, and (5) development of concepts for cutting instability control and machine-tool design applicable to high-speed cutting processes.

1.1 Instability in Turning Operation

We start the book with a comprehensive investigation on machining instability by employing a three-dimensional turning model [2, 3, 4, 5] that addresses the concerns that (1) cutting dynamic models developed to date all fall short of grasping the underlying dynamics of turning operation and (2) stability charts developed using the models are inadequate to identify the true stability regions. The specific objective of the study is to establish the proper interpretation of cutting instability so as to establish the knowledge base for cutting instability control.

The complex machining model describes the coupled tool–workpiece dynamics subject to nonlinear regenerative cutting forces, instantaneous depth-of-cut, and workpiece whirling due to material imbalance. In the model the workpiece is considered a system of three rotor sections – namely, unmachined, being machined, and machined – connected by a flexible shaft, thus enabling the motion of the workpiece relative to the tool and tool motion relative to the machining surface to be three-dimensionally established as functions of spindle speed, depth-of-cut, rate of material removal, and whirling. Figure 1.1 shows the configuration of the tool engaging the section that is being cut where the deviation of the geometric center from the center of mass constitutes the eccentricity that characterizes workpiece whirling. Using the model a rich set of nonlinear behaviors of both the tool and workpiece – including period-doubling bifurcation and chaos signifying the extent of machining instability at various depth-of-cuts – was observed. Results presented therein agree favorably with physical

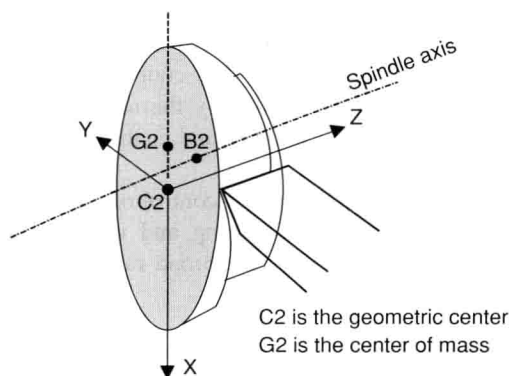


Figure 1.1 Configuration of the section that is being machined

experiments reported in the literature. It is found that at, and up to, certain ranges of depth-of-cuts, whirling is a non-negligible part of the fundamental characteristics of the machining dynamics. Contrary to common belief, whirling is found to have an insignificant impact on tool motions. The efforts documented in [2, 3, 4, 5] also show that the linearized turning model underestimates tool vibrations in the time domain and overestimates system behaviors in the frequency domain; whereas the nonlinear model agrees with the physical results reported in the literature in describing machining stability and chatter. The coupled workpiece–tool vibrations described by the nonlinear model are more pragmatic than the linearized counterpart in revealing the true machining state of motion. The model also reveals in the qualitative sense the broadband behavior of the tool natural frequency associated with unstable situations. Vibration amplitudes obtained using the linearized model, however, are diverging at certain depth-of-cuts (DOCs) without the commonly observed randomness in oscillation. Moreover, the linearized model deems instability at low DOCs and predicts a bifurcated state of unstable motion that is described as chaotic using physical data. Many important insights are gained using the model, including the fact that if the underlying dynamics of machining is to be established, and stability limits to be precisely identified, linearization of the nonlinear model is not advisable.

1.1.1 Impact of Coupled Whirling and Tool Geometry on Machining

In addition to speed, feed rate, and DOC that affect material removal rate (MRR) and determine cutting force and hence power consumption, tool geometry is also one of the prominent parameters that impacts machining productivity. Surface roughness, chip formation changes, and chip flow angle are also affected by tool geometry. Even though chip flow angle is related to tool angles, chip flow angle is a function only of DOC. Figure 1.2 gives a view of the rake angle, α , while undergoing cutting action. Tool rake angle determines the flow of the newly formed chip. Usually the angle is between $+5^\circ$ and -5° . To compare with the experimental result reported in [6], a constant spindle speed $\Omega = 1250$ rpm, a constant chip width $t_0 = 0.0965$ mm, and an eccentricity $\varepsilon_1 = 0.2$ mm are considered along with several different DOCs including $\text{DOC} = 1.62$ mm and 2.49 mm. The workpiece considered is a 4140 steel bar of 0.25 m length (l_0) and $r_3 = 20.095$ mm radius of the machined section. The starting location of the carbide tool is set at 0.15 m from the chuck. There are three types of plots in the figures found in the sections that follow. The top rows plot time histories, whereas the middle rows give their corresponding time-frequency responses obtained using instantaneous frequency (which will be covered in great detail in Chapter 4). The last rows show the Lyapunov spectra where the largest Lyapunov exponents are shown. Instantaneous frequency is employed to realize subtle features characteristic of machining instability.

Positive rake makes the tool sharp, but it also weakens the tool compared with negative rake. Negative rake is better for rough cutting. The selection of tool geometry depends on the particular workpiece and tool materials being considered. To establish that tool angle does have significant effects on cutting stability, two sets of tool geometries are used to determine the cutting force in the following. Their values are given in Table 1.1. Both sets are taken from the tool inserts that were used in the experiments reported in [6]. Since DOC considered in the numerical study is less than 1 mm and can be considered as non-rough cutting, rake angles are taken as positive for all cases. Note that negative rake is better for roughing. Three

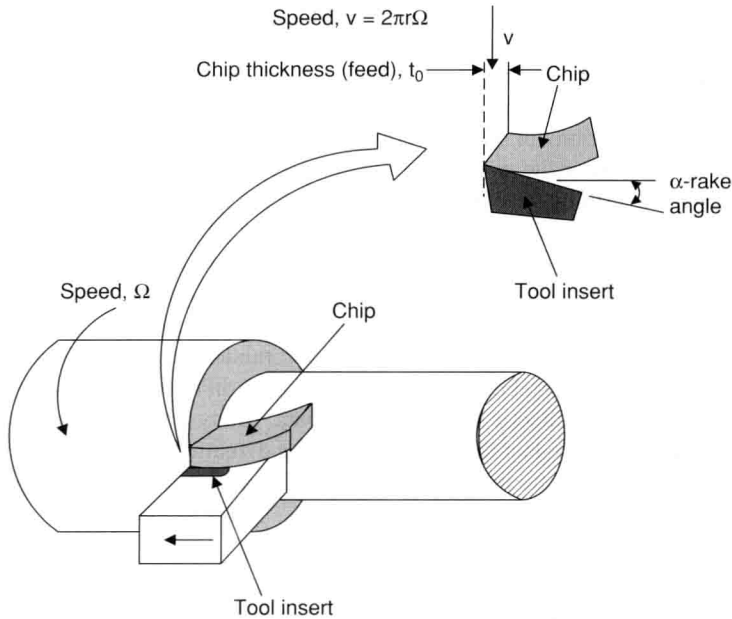


Figure 1.2 Cutting action with tool rake angle

DOCs (0.9 mm, 0.75 mm, and 0.5 mm) are used with a 1250 rpm spindle speed and a feed of 0.0965 mm per revolution in the study.

Except for Figures 1.6 and 1.7, all figures in Figures 1.3–1.8 give time responses, instantaneous frequency responses between 3 to 5 sec, and the corresponding Lyapunov spectra. X-direction system responses are examined to demonstrate workpiece behaviors, and Z-direction responses are analyzed to investigate tool motions. See also Figure 1.1 for the coordinates defined for the being-machined section. Plots in the right column correspond to Set #1 tool geometry conditions and the left column corresponds to Set #2 tool angles. In Figure 1.3, the X-direction vibration amplitude of Set #2 tool geometry is seen to be twice that of Set #1. However, their frequency domain behaviors are similar with a workpiece natural frequency at 3270 Hz and a whirling frequency at 20.8 Hz. Set #2 shows two more frequencies, one near the tool natural frequency at 425 Hz and another at 250 Hz, which disappears after 3.9 s. Set #1 has only one more tool-excited frequency. The frequency can be seen to decrease from 580 Hz to 460 Hz within 2 seconds, implying that tool geometry is a non-negligible parameter affecting workpiece stability.

Table 1.1 Tool angles

| Set Number | Side cutting edge angle | Rake angle | Inclination angle |
|------------|-------------------------|------------|-------------------|
| 1 | 45° | 3.55° | 3.55° |
| 2 | 15° | 5° | 0° |

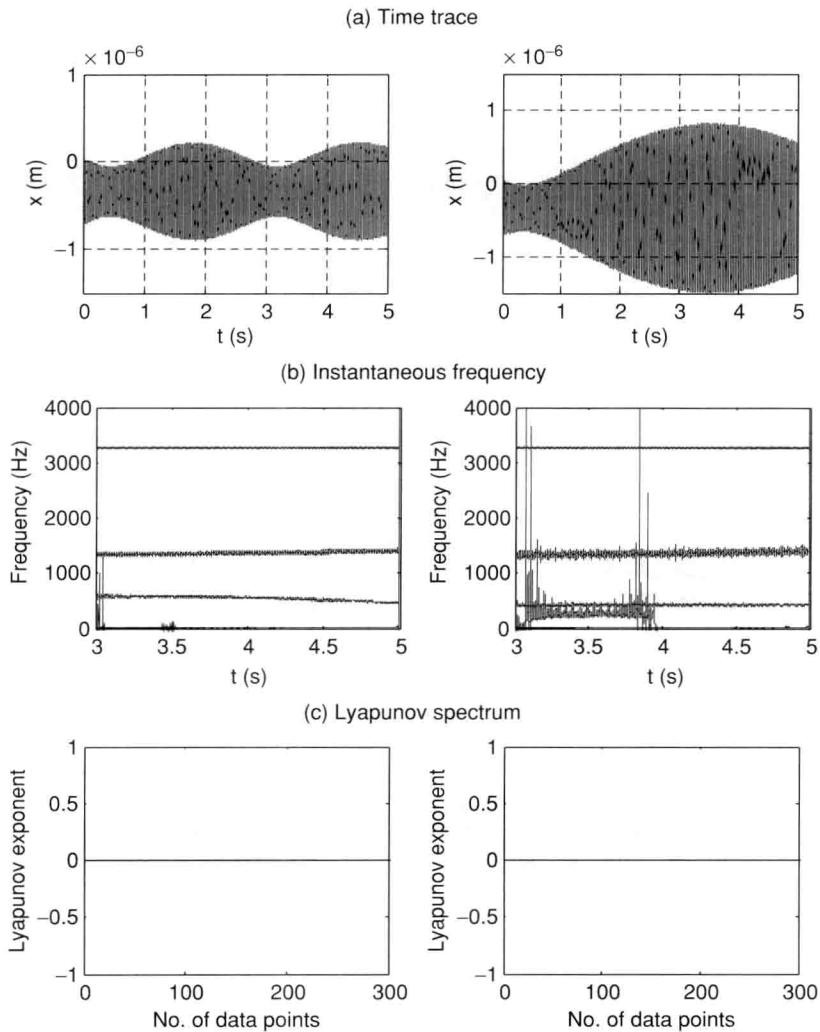


Figure 1.3 X-direction time responses, corresponding instantaneous frequency and Lyapunov spectra for Set #1(left) and Set #2 (right) for $\text{DOC} = 0.90$ mm at $\Omega = 1250$ rpm

When DOC is decreased to 0.75 mm in Figure 1.4, there are still differences in vibration amplitudes. With the reduction of its diameter, the workpiece natural frequency decreases to 3250 Hz. While whirling frequency remains the same, a 900 Hz component of a wide 500 Hz bandwidth dominates in both systems. It can be seen in Set #2 that a bifurcation of the tool-excited natural frequency at 425 Hz diminishes after 4.8 seconds. On the other hand, Set #1 does not have a bifurcation. It has a frequency component increase from 250 to 400 Hz. The frequency components then disappear afterward. Both Lyapunov spectra fluctuate near zero, thus leaving a question over whether the systems are exactly stable. Further decreasing DOC

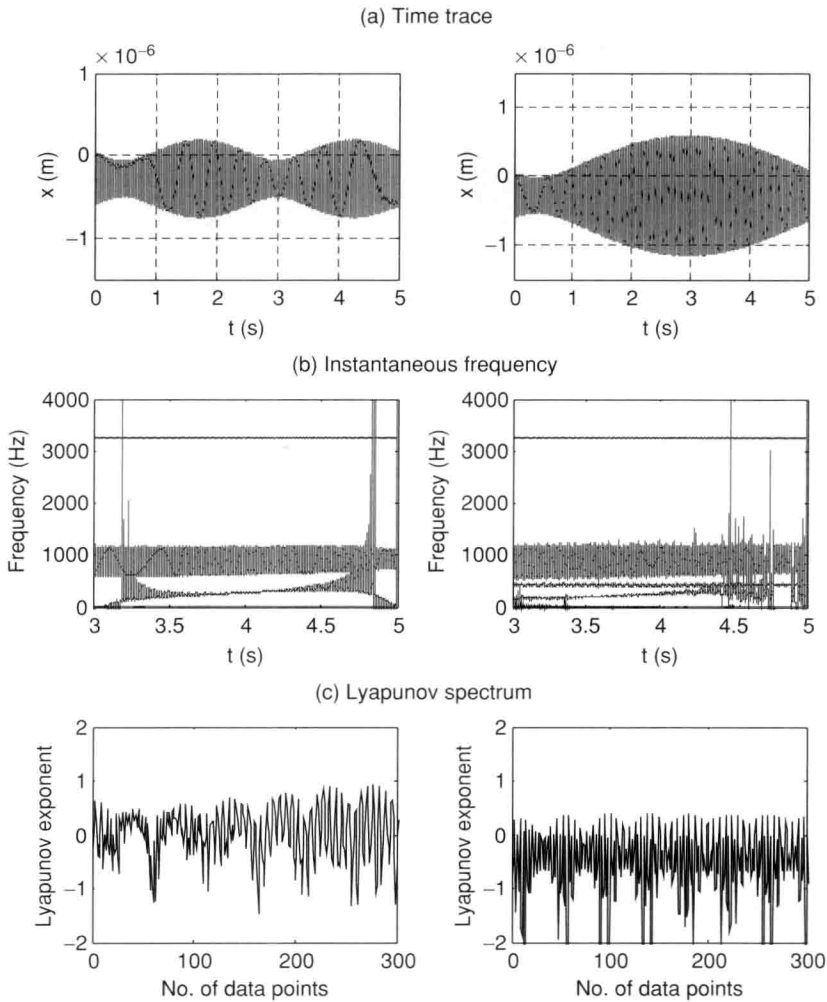


Figure 1.4 X-direction time responses, corresponding instantaneous frequency and Lyapunov spectra for Set #1(left) and Set #2 (right) for DOC = 0.75 mm at $\Omega = 1250$ rpm

to 0.5 mm in Figure 1.5 means both systems show an unstable situation marked by positive Lyapunov exponents.

The relatively large force fluctuation seen in Figure 1.6 explains the large vibration amplitudes seen for the tool geometry Set #2. Forces of large fluctuation push the workpiece to deflect more. It is interesting to note that, even though tool geometry variations are supposed to affect the cutting force, X-direction force amplitudes are almost identical for both tool geometry sets.

Effects of tool geometry can be seen in the Y- and Z-direction force components in Figure 1.7. While Y-direction forces for Set #2 are less than those of Set #1, Set #2 Z-direction forces are

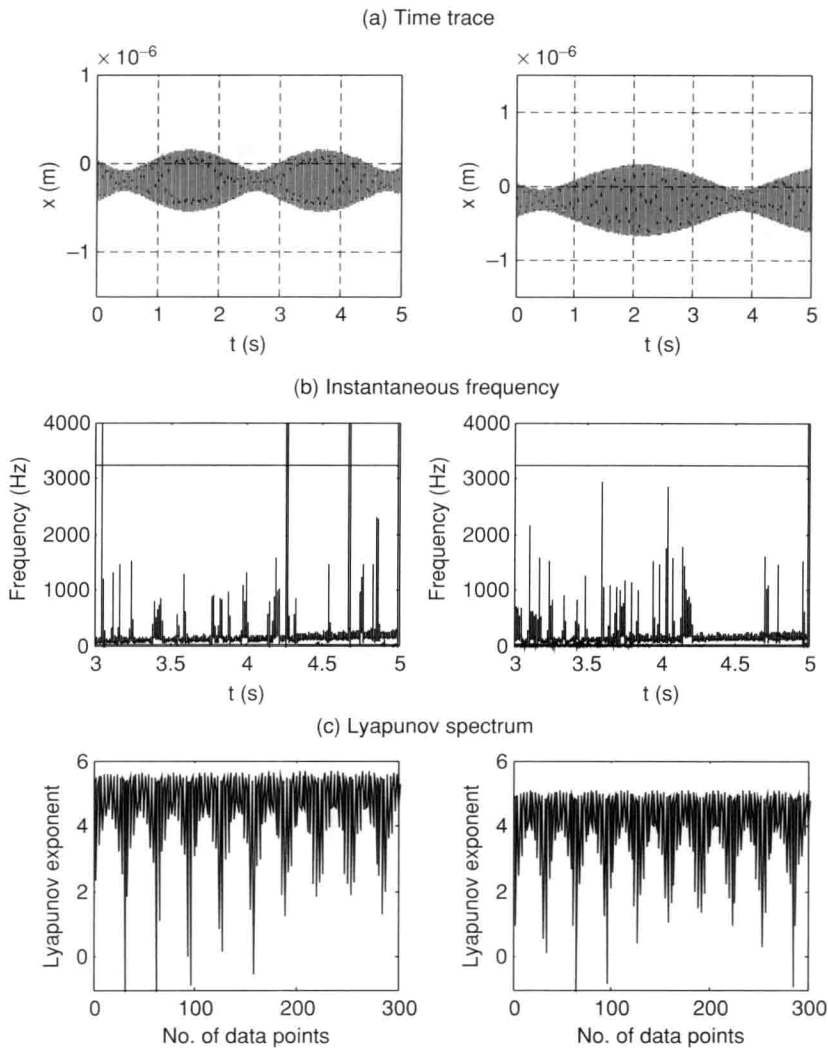


Figure 1.5 X-direction time responses, corresponding instantaneous frequency and Lyapunov spectra for Set #1(left) and Set #2 (right) for DOC = 0.50 mm at $\Omega = 1250$ rpm

much higher than those of Set #1. In all plots, it is seen that force responses associated with Set #1 tool geometry fluctuate less compared with those of Set #2. Tool dynamical motions for DOC = 0.9 mm, 0.75 mm, and 0.5mm are also considered. Even though force fluctuations and vibration amplitudes are both prominent, Set #2 is relatively more stable. Of the three DOCs considered, two behave dissimilarly. In all three cases, the vibration history of Set #1 has amplitudes that are of nanometers in scale. On the other hand, Set #2 vibrates with amplitudes that are a few microns for DOC = 0.9 mm and 0.75 mm, and several nanometers for DOC = 0.5 mm. Unlike Set #1, all Lyapunov spectra for Set #2 are evidence of a stable state of dynamic

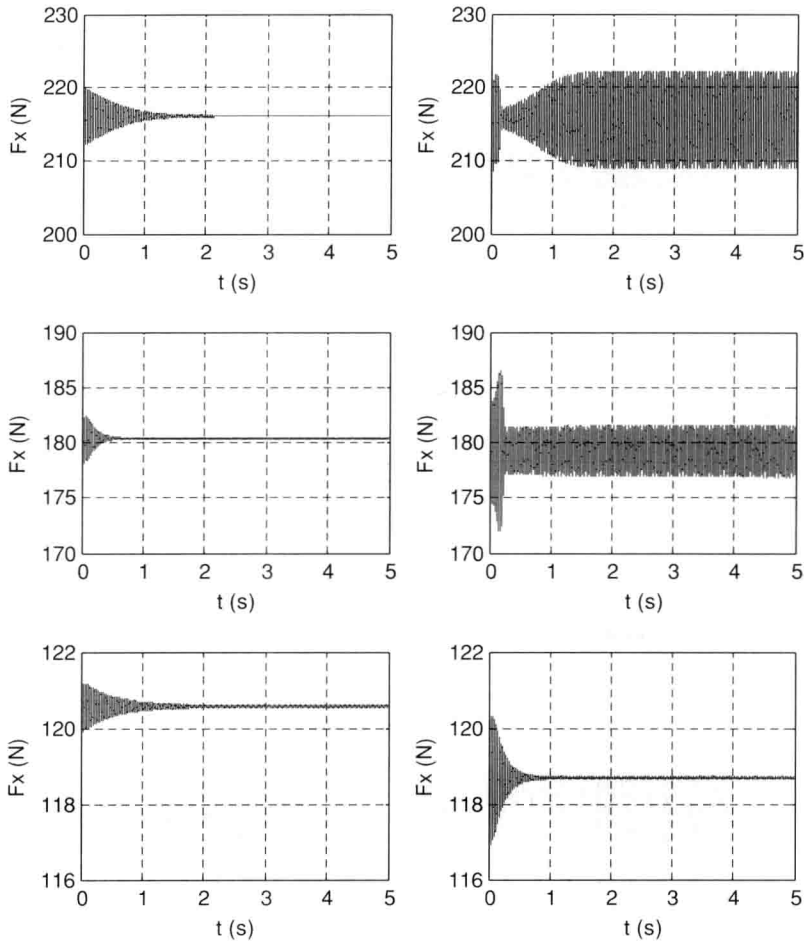


Figure 1.6 Forces in X- direction for Set #1(left) and Set #2 (right) for DOC = 0.90 mm (top), DOC = 0.75 mm (middle), and DOC = 0.50 mm (bottom) at $\Omega = 1250$ rpm

response. Though it has positive Lyapunov exponents, Set #2 shows instability for the DOC = 0.9 mm and 0.5 mm cases. IF plots for DOC = 0.9 mm in Figure 1.8 confirm that the Set #1 response is broadband and thus unstable, and Set #2 is stable with a clean spectrum. Although the Lyapunov spectrum indicates a stable state of tool motion for Set #1 at DOC = 0.75 mm, the corresponding instantaneous frequency suggests otherwise. The instantaneous frequency plot for Set #2 at DOC = 0.5 mm also contradicts the Lyapunov spectrum (not shown). A detailed review of the individual instantaneous frequency mono-components reveals that the frequency at 3240 Hz has bifurcated three times. Thus, it is in a highly bifurcated state.

The effects of tool geometry on cutting dynamics and its impact on surface finishing investigated above generate a few observations. The manufacturing industry has long learned to employ tool inserts with complex geometry to achieve better product surface finish. However,